

# Lawrence Berkeley National Laboratory

## LBL Publications

### Title

Insights into the Thermal Expansion of Amorphous Polymers

### Permalink

<https://escholarship.org/uc/item/43r5h86v>

### Journal

ACS Macro Letters, 13(11)

### ISSN

2161-1653

### Authors

Eim, Sungoh

Jo, Seungyun

Kim, Junsu

et al.

### Publication Date

2024-11-19

### DOI

10.1021/acsmacrolett.4c00574

### Copyright Information

This work is made available under the terms of a Creative Commons Attribution License, available at <https://creativecommons.org/licenses/by/4.0/>

Peer reviewed

# Thermal Molecular Expansion of Amorphous Polymers to Interpret Volume Expansion

*Sungoh Eim,<sup>†</sup> Seungyun Jo,<sup>†</sup> Junsu Kim,<sup>†</sup> Sungmin Park,<sup>‡</sup> Dongjun Lee,<sup>§</sup> Thomas P. Russell,<sup>\*,^</sup> and Du Yeol Ryu<sup>\*,†</sup>*

<sup>†</sup>Department of Chemical and Biomolecular Engineering, Yonsei University, 50 Yonsei-ro, Seodaemun-gu, Seoul 03722, Korea

<sup>‡</sup>Advanced Materials Division, Korea Research Institute of Chemical Technology, 141 Gajeong-ro, Yuseong-gu, Daejeon, 34114, Korea

<sup>§</sup> Sustainable Materials Research Team, Advanced Vehicle Platform Division, Hyundai Motor Group, 7, Cheoldobangmulgwan-ro, Uiwang, Gyeonggi-do, 16082, Korea

<sup>^</sup>Polymer Science & Engineering Department, Conte Center for Polymer Research, University of Massachusetts, 120 Governors Drive, Amherst, Massachusetts 01003, United States; Materials Sciences Division, Lawrence Berkeley National Laboratory, 1 Cyclotron Road, Berkeley, California 94720, United States

**KEYWORDS:** Homopolymer, Thermal volume expansion, Molecular distance

## **ABSTRACT**

We investigated the temperature dependence of molecular distances to corroborate thermal expansion of amorphous polystyrene (PS) and poly(methyl methacrylate) (PMMA) homopolymers. The strong correlation maxima observed in the wide-angle X-ray scattering (WAXS) profiles were distinct, and the peak shapes were maintained during heating of the sample to 250 °C, indicating the most probable molecular distances. The three characteristic peaks were attributed to inter- and intramolecular distances, owing to the multiple correlations between the backbone, substituents, and repeating units. For both PS and PMMA, a remarkable temperature dependence was identified for the largest molecular distances averaged from the intermolecular correlations. Based on the temperature dependence of molecular distances, the coefficients of molecular expansion were very close to the coefficients of thermal expansion. This study provides a simple yet accurate methodology to correlate macro-scale volume expansions with molecular expansion configured by the accessible WAXS data.

## INTRODUCTION

Thermal expansion is ubiquitously manifested in most materials and characterized by a decrease in density owing to an increase in volume with increasing temperature. Understanding thermal expansion is essential in engineering, materials science, and other disciplines because the dimensional stability of structures subjected to temperature variations affects component performance.<sup>1</sup> In metals, this expansion is normally isotropic and primarily occurs due to the increased movement of free electrons and lattice vibrations along the atomic lattices.<sup>2</sup> In contrast, the thermal expansion behavior of polymeric materials is substantially influenced by molecular structures, and it may reveal more significantly in certain directions associated with molecular orientation or crystallinity.<sup>3,4</sup> While often overlooked due to its seemingly trivial magnitude, it plays a crucial role in the long-term performance of plastic-containing devices and instruments across diverse industrial areas.<sup>5</sup> Even slight deviations in dimension arising from different thermal expansions might lead to undesired consequences such as cracks and warpage, debilitating the functionality and reliability associated with their critical systems.<sup>6,7</sup>

Amorphous polymers, unlike their crystalline counterparts, lack well-defined periodic molecular structures. Thus, their thermal expansion depends on the unique disorder-like characteristics, which primarily reflect an increase in average molecular distances. In particular, for structural polymer chains, thermal expansion along the main chain is inherently negligible because of the dominant presence of strong covalent bonds. However, the interchain expansion in favor of a perpendicular direction to the main chain is considerable because the polymer chains are weakly attracted by the molecular interactions such as Van der Waals forces,  $\pi$ - $\pi$  interactions, and hydrogen bonds. Upon elevation of temperature, the thermal energy intensifies

the vibrational mode of the rotational isomeric chains, resulting in a dominant expansion perpendicular to the main chain rather than in the parallel direction.<sup>4,8</sup>

Wide-angle X-ray scattering (WAXS) measurements have been widely used to accurately determine the correlations militated between the backbone, substituents, and repeating units. For amorphous polymers, relatively broad peaks over a wide range do not characterize a regular lattice but define the short-range-order correlations of polymer chains, which are caused by both inter- and intramolecular interactions. In this context, several studies on the structure and chain conformation of various amorphous polymers have highlighted the molecular distance associated with inter-and intrachain correlations.<sup>9-16</sup> However, little attention has been devoted to elucidating the thermal expansion behavior in terms of molecular expansion over a wide range of temperatures.

In this study, we address an unexplored question regarding the temperature dependence of molecular distances to corroborate the thermal expansion of amorphous polystyrene (PS) and poly(methyl methacrylate) (PMMA) homopolymers. We measured inter- and intramolecular distances using temperature-dependent WAXS experiments, and the obtained coefficients of molecular expansion were compared with those of thermal expansion (CTEs) measured by ellipsometric spectroscopy. Our methodological approach to thermal expansion provides fundamental insights into the temperature dependence of molecular distances to elucidate the thermal characteristics of amorphous polymers.

## **EXPERIMENTAL SECTION**

### **Synthesis and chemical characterization**

PS and PMMA were synthesized via living anionic polymerization of each monomer in tetrahydrofuran (THF) at  $-78\text{ }^{\circ}\text{C}$  under purified argon. These reactions for the PS and PMMA were initiated using sec-butyllithium (1.3 M, Aldrich) and sec-butyllithium coupled with 1,1-diphenylethylene in the presence of LiCl (high purity, Aldrich), respectively. THF was purified using a set of activated alumina and copper-oxide columns to ensure oxygen- and water-free conditions. Monomers degassed with  $\text{CaH}_2$  (Aldrich) were vacuum-distilled over the second purifiers of dried dibutylmagnesium and trioctylaluminum for styrene and methacrylate, respectively. The polymer solution terminated with isopropyl alcohol was precipitated in an excess methanol/water (80/20 by wt %) solution. The powder samples retrieved from a filtration step were first dried at room temperature under vacuum. Then, the temperature was elevated to  $150\text{ }^{\circ}\text{C}$  for 48 h.

The number-average molecular weights ( $M_n$ ) of PS and PMMA were characterized to be 51,000 and 30,800 Da, respectively, with a narrow dispersity ( $D = M_w/M_n$ ) less than 1.04, as analyzed using size-exclusion chromatography (SEC) (Figure S1). Differential scanning calorimetry (DSC: PerkinElmer Diamond DSC) was conducted at a heating rate of  $20\text{ }^{\circ}\text{C}/\text{min}$  from 50 to  $250\text{ }^{\circ}\text{C}$ . Glass transition temperature ( $T_g$ ) of the PS and PMMA were evaluated to be 104 and  $125\text{ }^{\circ}\text{C}$ , respectively, measured during the second heating run (Figure S1).

### **Wide-angle X-ray Scattering (WAXS)**

The WAXS experiments were performed at the Pohang Accelerator Laboratory (4C and 9A beamlines), Korea. The operating conditions for the 4C and 9A beamlines were set at the wavelength of  $\lambda = 0.733$  and  $0.626\text{ \AA}$ , respectively, a typical beam size of  $0.8\text{ mm} \times 0.8\text{ mm}$ , a sample-to-detector distance (SDD) of 0.2 m, and exposure times of 1–10 s. A two-dimensional (2D) Mar CCD camera (Rayonix LLC., Marccd-165) was used to collect the scattered intensities.

The scattering patterns were collected at various temperatures and azimuthally integrated to produce one-dimensional (1D) WAXS intensity profiles as functions of the scattering vector  $q$ .

### **Thermal behavior of Homopolymers**

Solutions of PS and PMMA in toluene were spin-coated onto a standard Si substrate (with a 2-nm oxide layer) typically at 1500 to 3000 rpm for 60 s, and the films were thermally annealed at 150 °C under vacuum for 24 h. The films were prepared with a thickness greater than 300 nm, in which the physical properties of the films are presumed to be close to those of the bulk state.<sup>17,18</sup> For ellipsometry measurements, halogen and deuterium UV-Vis light sources were cooperatively used for the PS films to access a wide range of  $\lambda$  from 150 to 850 nm (or 1.5 – 5.0 eV), whereas for the PMMA films a halogen source was applied to cover  $\lambda$  from 350 to 850 nm (or 1.5 – 3.5 eV). A lab-made heating stage was installed in the spectroscopic ellipsometry (SEMG-1000, Nanoview Co., Korea) to obtain two ellipsometric angles ( $\Psi$  and  $\delta$ ) as a function of temperature. To evaluate the thermal expansion of the homopolymer films, *in-situ* heating experiments were carried out from 30 to 250 °C at a rate of 2.0 °C/min under vacuum.

## **RESULTS AND DISCUSSION**

Anionic polymerization was used to prepare well-defined amorphous PS and PMMA homopolymers with narrow dispersities less than 1.04. The PS and PMMA samples were pre-annealed at constant temperatures of 140 and 160 °C under vacuum, respectively, above their  $T_g$ s (104 and 125 °C of PS and PMMA, respectively) to ensure an equilibrium state prior to measurement. The WAXS experiments were carried out for structural characterization and the scattering patterns were collected from 30 to 250 °C during heating at a rate of 2.0 °C/min. The measurements were conducted in an N<sub>2</sub> environment to suppress the thermal degradation of the

samples at high temperatures. For the PS, a 2D WAXS pattern (inset of [Figure 1a](#)) measured at 30 °C exhibits the three distinct amorphous halo rings, indicating that the structure lacks long-range periodic molecular order. By azimuthally integrating the 2D data measured at various temperatures, we obtained the 1D WAXS intensity profiles of the PS ([Figure 1a](#)) as a function of the scattering vector  $q = (4\pi/\lambda)\sin\theta$ , where  $2\theta$  and  $\lambda$  are the scattering angle and wavelength of the incident X-ray beam, respectively. The three characteristic peaks identified at 0.72, 1.37, and 2.95 Å<sup>-1</sup> (denoted as  $q_a$ ,  $q_b$ , and  $q_d$ , respectively) are distinct and maintain their peak shapes when the sample is heated to 250 °C. These peaks correspond to  $d$ -spacings of 8.61, 4.56, and 2.13 Å, respectively, by Bragg's law ( $d = 2\pi/q$ ).

The peaks of the PS are attributed to combinations of inter- and intramolecular distances between the backbone, phenyl, and repeating units ([Figure 1b](#)), according to molecular dynamics simulations for the PS.<sup>9,15,16</sup> The first peak ( $q_a$ ) represents a large molecular distance, averaged primarily from the intermolecular distances of backbone-backbone and backbone-phenyl. The second peak ( $q_b$ ) indicates an intermolecular phenyl-phenyl distance in major, although it also includes minor contributions from the intramolecular phenyl-phenyl and intermolecular backbone-phenyl distances. Interestingly, the highest intensity was observed in  $q_b$ , likely because the phenyl-phenyl correlations have a higher electron density than the others. In Particular, the contributions from the intermolecular backbone-phenyl distance affect both  $q_a$  and  $q_b$  because this distance spatially falls between the intermolecular distances of phenyl-phenyl and backbone-backbone.<sup>16</sup> The third broad maximum ( $q_d$ ) corresponds to a repeating-unit distance averaged from the carbon-second carbon distances along the backbone chains, which have the smallest correlation size in the polymer chains.

[Figure 1c](#) shows the molecular distance ( $d$ ) as a function of temperature, where the temperature-dependent  $d$  values are normalized by each initial  $d_0$ . Interestingly, remarkable



temperature dependence was observed specifically for the intermolecular distances ( $d_a$ ). The thermal energy intensifies the vibrational modes of the rotational isomeric chains, enabling a remarkable increase in  $d_a$  associated with weak interactions such as Van der Waals forces and  $\pi$ - $\pi$  interactions. As temperature increases, the  $T_g$  of PS was determined to be 105 °C at the intersection of the glassy and rubbery temperature ranges; this was very close to that (104 °C) measured by the DSC experiment. A similar trend was observed for the phenyl-phenyl molecular distance ( $d_b$ ), although the temperature dependence was lower than that of  $d_a$ . However, the repeating-unit distance ( $d_a$ ) remains unchanged regardless of the increase in temperature because of the dominant presence of strong covalent bonds. Note that above the  $T_g$  of the PS, a slight increase in the intensity of  $q_a$  with increasing temperature is not indicative of increasing molecular order but the consequence of the shift in  $q_a$  toward lower- $q$  (Figure S2).<sup>16</sup>

The 2D WAXS pattern of the PMMA (inset of Figure 2a) measured at 30 °C displays the three distinct amorphous halo rings. The three characteristic peaks at 0.94, 2.15, and 2.96 Å<sup>-1</sup> (denoted as  $q_a$ ,  $q_c$ , and  $q_d$ , respectively) (Figure 2a), corresponding to  $d$ -spacings of 6.40, 2.92, and 2.12 Å, respectively, are attributed to the nonperiodic, short-range molecular order. As temperature increases to 250 °C, the three peaks show a trend similar to the peaks of the PS. The first peak ( $q_a$ ) represents a large molecular distance, averaged primarily from the intermolecular distances of backbone-backbone, backbone-ester, and backbone-methyl (Figure 2b). It should be noted that a small shoulder peak ( $q_b = 1.24$  Å<sup>-1</sup>) on the right side of the first peak is attributed to the intramolecular ester-ester distance ( $d_b = 5.06$  Å) though in minor (Figure S3).<sup>13</sup> The second peak ( $q_c$ ) represents an intramolecular methyl-methyl distance (or a smaller-scale ester-ester distance), while the third broad maximum ( $q_d$ ) corresponds to an average repeating-unit distance, similar to that ( $d_a = 2.13$  Å) of the PS. Figure 2c shows each molecular distance ( $d$ ) with increasing temperature. The intermolecular distances ( $d_a$ ) exhibit a strong temperature dependence. As

temperature increases, the  $T_g$  of PMMA was determined to be 125 °C, which was the same as that (125 °C) measured by the DSC experiment. However, the intramolecular distance of methyl-methyl ( $d_c$ ) slightly increases above the  $T_g$ , whereas the repeating-unit distance ( $d_d$ ) remains nearly independent of temperature.

As manifested in the PS and PMMA, thermal expansion occurs predominantly perpendicular to the main chain rather than parallel, which is caused by a decrease in Van der Waals molecular interactions. In amorphous polymers, numerous chains are randomly entangled and radial thermal expansion of the entire chain occurs, in which the short-range-order molecular expansion would be associated with inter- and intramolecular distances. In a framework that the strong correlation maxima in the WAXS data reflect the most probable molecular distances, the molecular volume can be reasonably determined using the three distinct average distances. The apparent molecular volume ( $V$ ) was evaluated by  $d_a \times d_b \times d_d$  and  $d_a \times d_c \times d_d$  for the PS and PMMA, respectively (Figure 3a). The  $V$  was normalized by each initial  $V_0$  measured at 30 °C and plotted as a function of temperature (Figure 3b). The two different slopes below and above  $T_g$  were evident for the PS and PMMA, and the  $T_g$ s were determined from the intersection of the slopes, as denoted by the red arrows. These slopes corresponding to the glassy and rubbery states were defined as the coefficient of molecular expansion (CME) for the amorphous polymers. The CMEs for the PS were determined to be  $2.45 \times 10^{-4}/^\circ\text{C}$  below  $T_g$  and  $6.67 \times 10^{-4}/^\circ\text{C}$  above  $T_g$ , whereas for the PMMA, the CMEs were  $1.59 \times 10^{-4}/^\circ\text{C}$  below  $T_g$  and  $6.98 \times 10^{-4}/^\circ\text{C}$  above  $T_g$ .

For the experimental volume expansions, the films were prepared with a thickness greater than 300 nm (307 and 310 nm of the PS and PMMA, respectively), in which the physical properties of the films are presumed to be close to those of the bulk state. Ellipsometry was used to measure film thicknesses of the samples, where the thicknesses were collected from 30 to 250 °C during heating at a rate of 2.0 °C/min (Figure 3c). In the film geometry, the normalized film

thickness ( $h/h_0$ ) can be directly correlated to the volume change ( $V/V_0$ ), since the polymer chain expands vertically but not laterally due to a greater surface area ( $1.0 \text{ cm} \times 1.0 \text{ cm}$ ) than the thickness.<sup>17,19</sup> The CTEs of the glassy and rubbery states of the samples (the  $\alpha_g$  and  $\alpha_r$  values, respectively) were characterized below and above  $T_g$ , respectively, leading to the  $T_g$ s of 104 and 124 °C for the PS and PMMA, respectively. The CTEs obtained from the ellipsometry measurements were evaluated to be  $\alpha_g = 2.09 \times 10^{-4}/^\circ\text{C}$  below  $T_g$  and  $\alpha_r = 6.48 \times 10^{-4}/^\circ\text{C}$  above  $T_g$  for the PS, and  $\alpha_g = 1.98 \times 10^{-4}/^\circ\text{C}$  below  $T_g$  and  $\alpha_r = 6.27 \times 10^{-4}/^\circ\text{C}$  above  $T_g$  for the PMMA. These values are similar to the values reported previously,<sup>17, 18, 20</sup> although the  $\alpha_r$  values of the PS and PMMA decrease with decreasing film thickness due to the long-range interactions from the substrates (Figure S4). Surprisingly, the CMEs obtained from the WAXS results for the PS and PMMA were found to be highly reliable and consistent with the CTEs within the experimental error ranges. Our results demonstrate that the characteristic peaks identified in the WAXS are average distances that encompass all the correlation distances interoperated in the polymer chains.

## CONCLUSION

We explored the molecular distances for the two amorphous polymers of PS and PMMA using the WAXS measurements. Owing to the loss of molecular periodicity, the short-range-order correlations of the polymer chains were unique and sufficient to represent the dominant inter- and intramolecular interactions between the backbone, substituents, and repeating units. For the three characteristic peaks of both PS and PMMA, the average inter- and intramolecular distances were extracted to compare their temperature dependences. Remarkable temperature dependence was identified for the largest molecular distances averaged from the intermolecular distances, although very weak and negligible for the intramolecular and repeating-unit distances.

Because it is reasonable to believe that the strong correlation maxima observed in the WAXS intensity profiles reflect the most probable molecular distances, the normalized molecular volume ( $V/V_0$ ) was characterized as functions of temperature. The CMEs derived from the WAXS results for the PS and PMMA were highly reliable and consistent with the CTEs quantified by volume measurements. Our approach, which correlates molecular- and macro-scale volume expansions, can provide an easy and straightforward methodology to predict the CTEs of amorphous polymers based on the accessible correlation distances interoperated in the polymer chains.

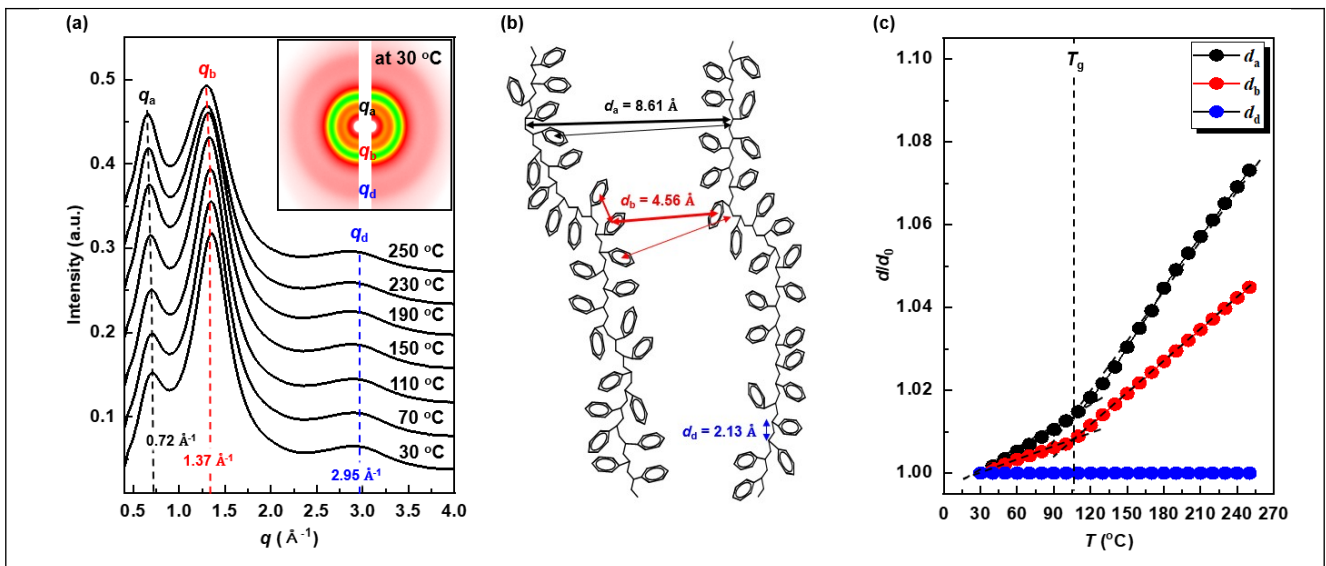


**Figure 1.** (a) WAXS intensity profiles of PS during heating at a rate of 2.0 °C /min from 30 to 250 °C, where the intensities were shifted by a factor of 0.04 to avoid overlap. The dashed lines denote  $q_a$  (black),  $q_b$  (red), and  $q_d$  (blue). The inset displays the 2D WAXS pattern measured at 30 °C. (b) Schematic illustration of various correlation contributions and average molecular distances ( $d_a$ ,  $d_b$  and  $d_d$ ) along the PS chains. (c) Molecular distance ( $d/d_0$ ) as a function of temperature, where the temperature-dependent  $d$  values are normalized by each initial  $d_0$  measured at 30 °C.

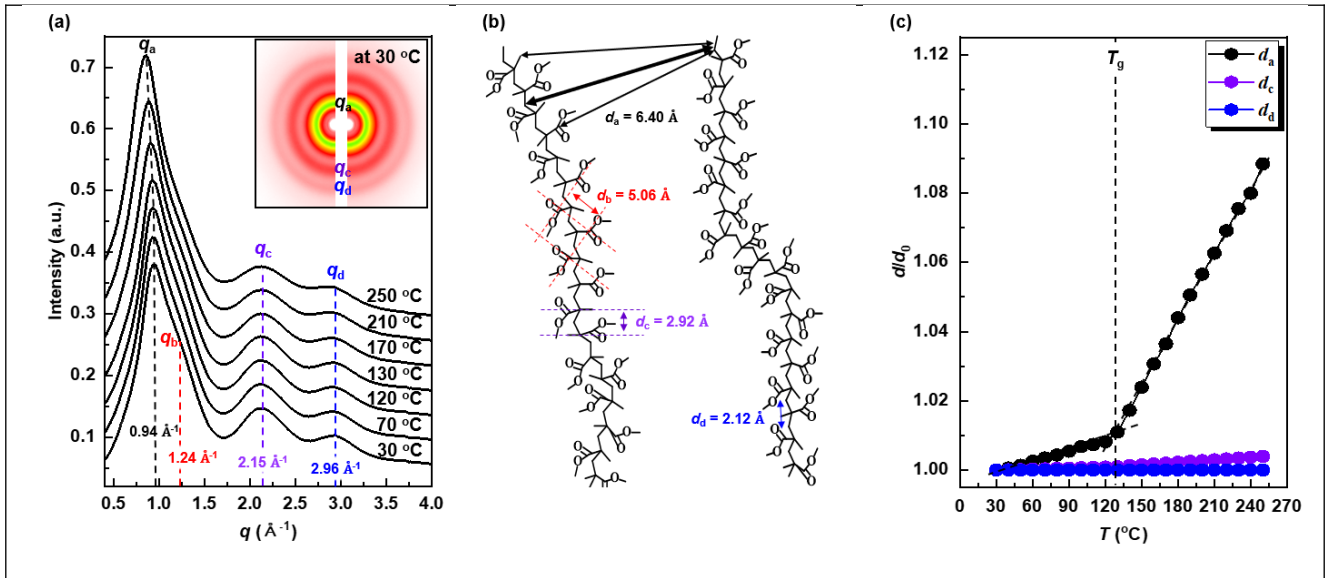


**Figure 2.** (a) WAXS intensity profiles of PMMA during heating at a rate of 2.0 °C /min from 30 to 250 °C, where the intensities were shifted by a factor of 0.04 to avoid overlap. The dashed lines denote  $q_a$  (black),  $q_b$  (red),  $q_c$  (purple), and  $q_d$  (blue). The inset displays a 2D WAXS pattern measured at 30 °C. (b) Schematic illustration of various correlation contributions and average molecular distances ( $d_a$ ,  $d_b$ ,  $d_c$ , and  $d_d$ ) along the PMMA chains. (c) Molecular distance ( $d/d_0$ ) as a function of temperature, where the temperature-dependent  $d$  are normalized by each initial  $d_0$  measured at 30 °C.

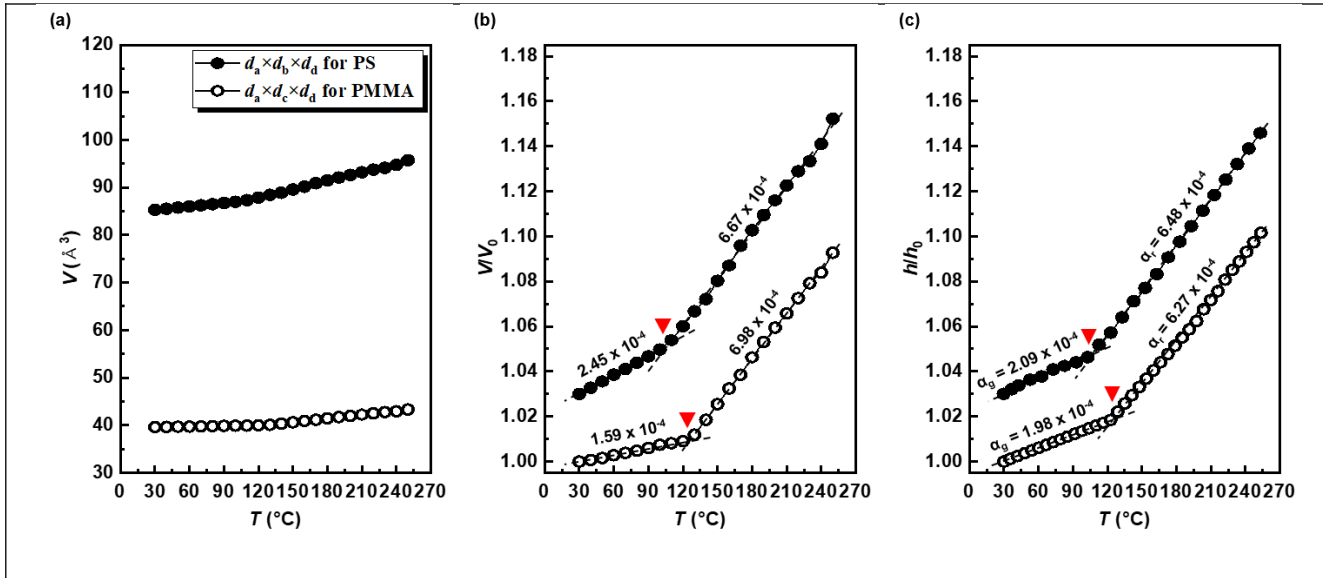


**Figure 3.** (a) Apparent molecular volume ( $V$ ) evaluated from  $d_a \times d_b \times d_d$  and  $d_a \times d_c \times d_d$  for the PS and PMMA, respectively. (b) Molecular volume ( $V/V_0$ ) as a function of temperature, where the temperature-dependent  $V$  were normalized by each initial  $V_0$  measured at 30 °C. The PS data was shifted by a factor of 0.03 to avoid overlap. The two different slopes below and above  $T_g$  (denoted by the red arrows) are defined as the coefficient of molecular expansion (CME) for amorphous polymers. (c) Film thickness ( $h/h_0$ ) as a function of temperature, where the temperature-dependent  $h$  were normalized by each initial  $h_0 = 307$  and 310 nm measured at 30 °C for the PS and PMMA, respectively. The temperature dependence of  $h/h_0$  corresponds to the coefficient of thermal expansion (CTE) obtained from the ellipsometry measurements, providing the CTEs of the glassy and rubbery states of the samples (the  $\alpha_g$  and  $\alpha_r$  values, respectively).

## ASSOCIATED CONTENT

### Supporting Information.

The Supporting Information is available free of charge at

<https://pubs.acs.org/doi/xxx/acs.macromol.xxx>.

SEC chromatograms, DSC data, and other relevant data (PDF)

## AUTHOR INFORMATION

### Corresponding Authors

**\*Thomas P. Russell**, *Polymer Science and Engineering Department, University of Massachusetts Amherst, 120 Governors Drive, Amherst, Massachusetts 01003, United States; Materials Science Division, Lawrence Berkeley National Laboratory, 1 Cyclotron Road, Berkeley, California 94720, United States; Orcid*<https://orcid.org/0000-0001-6384-5826>; Email: russell@mail.pse.umass.edu

**\*Du Yeol Ryu**, *Department of Chemical and Biomolecular Engineering, Yonsei University, 50 Yonsei-ro, Seodaemun-gu, Seoul 03722, Korea; E-mail: dyryu@yonsei.ac.kr*

### Authors

**Sungoh Eim**, *Department of Chemical and Biomolecular Engineering, Yonsei University, 50 Yonsei-ro, Seodaemun-gu, Seoul 03722, Korea*

**Seungyun Jo**, *Department of Chemical and Biomolecular Engineering, Yonsei University, 50 Yonsei-ro, Seodaemun-gu, Seoul 03722, Korea*

**Junsu Kim**, *Department of Chemical and Biomolecular Engineering, Yonsei University, 50 Yonsei-ro, Seodaemun-gu, Seoul 03722, Korea*

**Sungmin Park**, *Advanced Materials Division, Korea Research Institute of Chemical Technology, 141 Gajeong-ro, Yuseong-gu, Daejeon, 34114, Korea*



**Dongjun Lee**, *Sustainable Materials Research Team, Advanced Vehicle Platform Division, Hyundai Motor Group, 7, Cheoldobangmulgwan-ro, Uiwang, Gyeonggi-do, 16082, Korea*

### **Author Contributions**

-

### **Notes**

The authors declare no competing financial interest.

### **ACKNOWLEDGMENT**

This work was supported by the Hyundai Motor Group and the NRF Grants (2021R1A2C2006588, 2022R1A4A1020543) funded by the Ministry of Science, ICT & Future Planning (MSIP), Korea.

### **REFERENCES**

- (1) Callister, W. D. *Materials Science and Engineering: An Introduction, 10th Edition* WileyPLUS Card with EPUB Reg Card and Bridged Loose-Leaf Print Companion Set; Wiley, **2017**.
- (2) Quong, A. A.; Liu, A. Y. First-principles calculations of the thermal expansion of metals. *Physical Review B* **1997**, 56 (13), 7767-7770.
- (3) Van Krevelen, D. W.; Te Nijenhuis, K. Chapter 4 - Volumetric Properties. In *Properties of Polymers (Fourth Edition)*, Van Krevelen, D. W., Te Nijenhuis, K. Eds.; Elsevier, **2009**; 71-108.
- (4) Lacks, D. J.; Rutledge, G. C. Thermal expansion and temperature dependence of elastic moduli of aromatic polyamides. *Macromolecules* **1994**, 27 (24), 7197-7204.

- (5) Zhang, Q.; Wu, G.; Jiang, L.; Chen, G. Thermal expansion and dimensional stability of Al–Si matrix composite reinforced with high content SiC. *Materials Chemistry and Physics* **2003**, *82* (3), 780-785.
- (6) Multicomponent Polymeric Materials. In *Introduction to Physical Polymer Science*, **2005**; 687-756.
- (7) Yamada, S. A Mechanism for Board Warpage by Thermal Expansion of Surface Mounted Connector. *IEEE Transactions on Components, Hybrids, and Manufacturing Technology* **1986**, *9* (4), 508-512.
- (8) Ishige, R.; Masuda, T.; Kozaki, Y.; Fujiwara, E.; Okada, T.; Ando, S. Precise Analysis of Thermal Volume Expansion of Crystal Lattice for Fully Aromatic Crystalline Polyimides by X-ray Diffraction Method: Relationship between Molecular Structure and Linear/Volumetric Thermal Expansion. *Macromolecules* **2017**, *50* (5), 2112-2123.
- (9) Katz, J. R. X-ray spectrography of polymers and in particular those having a rubber-like extensibility. *Transactions of the Faraday Society* **1936**, *32* (0), 77-94.
- (10) Lovell, R.; Windle, A. H. Analysis of wide-angle X-ray diffraction patterns of aligned glassy polymers with particular references to polystyrene. *Polymer* **1976**, *17* (6), 488-494.
- (11) Adams, R.; Balyuzi, H. H. M.; Burge, R. E. The structure of amorphous polystyrene by X-ray scattering and simple conformational analysis. *Journal of Materials Science* **1978**, *13* (2), 391-401.
- (12) Atkins, E. D. T.; Keller, A.; Shapiro, J. S.; Lemstra, P. J. Extended-chain structure for isotactic polystyrene: additional X-ray diffraction and calorimetric results. *Polymer* **1981**, *22* (9), 1161-1164.
- (13) Lovell, R.; Windle, A. H. Determination of the local conformation of PMMA from wide-angle X-ray scattering. *Polymer* **1981**, *22* (2), 175-184.

- (14) Mitchell, G. R.; Windle, A. H. Conformational analysis of oriented non-crystalline polymers using wide angle X-ray scattering. *Colloid and Polymer Science* **1982**, *260* (8), 754-761.
- (15) Mitchell, G. R.; Windle, A. H. Structure of polystyrene glasses. *Polymer* **1984**, *25* (7), 906-920.
- (16) Ayyagari, C.; Bedrov, D.; Smith, G. D. Structure of Atactic Polystyrene: A Molecular Dynamics Simulation Study. *Macromolecules* **2000**, *33* (16), 6194-6199.
- (17) Shin, Y.; Lee, H.; Lee, W.; Ryu, D. Y. Glass Transition and Thermal Expansion Behavior of Polystyrene Films Supported on Polystyrene-Grafted Substrates. *Macromolecules* **2016**, *49* (14), 5291-5296.
- (18) Lee, S.; Lee, W.; Yamada, N. L.; Tanaka, K.; Kim, J. H.; Lee, H.; Ryu, D. Y. Instability of Polystyrene Film and Thermal Behaviors Mediated by Unfavorable Silicon Oxide Interlayer. *Macromolecules* **2019**, *52* (19), 7524-7530.
- (19) Lee, D. H.; Lee, H.; Lee, Y.; Kim, Y.; Ryu, D. Y. Enthalpic and Volumetric Changes at Phase Transitions of Polystyrene-b-poly(alkyl methacrylate) Copolymers and Their Pressure Dependence. *Macromolecules* **2014**, *47* (6), 2169-2173.